International Journal of Computing and Digital Systems
ISSN (2210-142X)
Int. J. Com. Dig. Sys. 12, No.1 (Jul-2022)

https://dx.doi.org/10.12785/ijcds/120119

Analysis of the Fifth Generation NOMA System Using LSTM Algorithm

Abhishek Bhatt[1], Ravi Shankar[2], Gniewko Niedbala[3] and Ajay Rupani[4]

[1]*College of Engineering, Pune, India*
[2]*Student Member, IEEE, India*
[3]*Poznan University of Life Sciences, Poland*
[4]*Manipal University Jaipur, India*

Received 3 Jun. 2021, Revised 31 Mar. 2022, Accepted 18 Jun. 2022, Published 1 Jul. 2022

Abstract: This study investigates non-orthogonal multiple access (NOMA) receivers based on deep learning (DL) employing the long-short term memory technique (LSTM) over frequency-flat Rayleigh distributed fading links. The fading links are independently and identically distributed (i.i.d.). When comparing the DL-based NOMA receiver's system performance to that of the traditional NOMA technique, the DL-based receiver surpasses the conventional successive interference cancellation (SIC)-based NOMA receiver. The simulations are conducted for various values of cyclic prefix (CP) considering the clipping noise (CN) under real-time propagation characteristics. It has been discovered that neither minimum mean square error (MMSE) nor least square error (LSE) can provide precise information on fading channel coefficients. With a signal-to-noise ratio (SNR) value exceeding 14 dB, precision tends to be saturated. On the other hand, DL techniques continue to be effective in channel estimation and detection. Lower learning rates improve system performance, whereas a high learning rate generates rapid changes in the weights of the DL NOMA detector, leading to a very high validation error value.

Keywords: deep reinforcement learning (DRL), mixed-integer nonlinear programming (MINLP), additive white Gaussian noise (AWGN), Fourier transform (FT), fifth generation (5G).

1. Introduction

5G and beyond-5G (B5G) wireless networks will deliver higher spectral efficiency (SE) by increasing spectrum utilization from sub-3 GHz in the 4th generation (4G) to 150 GHz and beyond. 5G may operate at sub-6 GHz and 30 GHz and higher, bringing high channel capacity (near Shannon rate), multi-Gbps speed, and extremely low latency [1], [2]. Compared to 4G, the new 5G network offers improved speed, capacity, bandwidth, availability, coverage, and lower latency. Improving these networks will significantly impact the way people around the world live, work, and play. 5G will help smart homes and smart cities evolve further. Edge computing will expand the use of machine learning (ML) into previously unseen areas [3], [4]. From smart cities that provide increased energy harvesting (EH) schemes to smart traffic lights that change patterns based on traffic, 5G applications that rely on higher network capacity and lower latency will influence practically everyone. With an increasing number of user-equipments (UEs), communication systems will certainly become overloaded with high volumes of data traffic in the future. Current multiple access (MA) schemes will most likely be incapable of serving efficiently in enormously overloaded environments. SE has recently been identified as a promising approach for 5G and B5G communications that may boost SE to a higher extent while servicing many users. NOMA uses the same resource blocks to service numerous users who are divided in their power domain at the same time. At the transmitter end of NOMA, superposition coding (SC) is employed, while SIC is given at the reception end. Mutual interference among users at the receiver end is not an issue with the classic orthogonal carrier-based technique (such as orthogonal multiple access (OMA) or orthogonal frequency division multiple access (OFDMA). Even with a modest receiver, it can improve system performance, but it cannot meet the 5G and B5G criteria, including improved end-to-end reliability, increased energy efficiency (EE) and SE, low latency, and massive connectivity. The primary purpose of NOMA is to give MA to numerous people at the same time, at the same frequency, and in the same location. Latency refers to the amount of time it takes for a signal to travel from its source to its receiver and back. Reduced latency has been one of the goals of each wireless generation. Data transmission will take less than 5 milliseconds (ms) round-trip on B5G networks, which will be even faster than 4G long-term evolution (LTE) [5], [6], [7]. 5G will have a latency far lower than human eyesight, enabling near-real-time remote operation

E-mail address: ravishankar.nitp@gmail.com

of devices. Many new applications will rely on machine-to-machine (M2M) communication that is not bound by human reaction time, which will become a limiting issue for remote 5G and internet of things (IoT) applications [8], [9]. While lower latency will benefit device-to-device (D2D) communication, multimedia applications, and Vehicle-to-vehicle (V2V) communication, online gaming applications are also anticipating 5G adoption. The combination of high-channel SE and EE is perfect for augmented reality (AR) and virtual reality (VR) applications, which are predicted to become more popular as the internet connection data rate improves, allowing for a more seamless, immersive experience [10]. While speed is appealing, experts and industry executives are concerned about the 5G network's ability to help organizations grow their digital activities. The data rate of 5G and B5G networks will be 1,000 times that of 4G, opening the path for IoT expansion. 5G in conjunction with IoT is a perfect combination, and they are about to revolutionize how people use wireless networks and the internet [11]. Multi-carrier NOMA, along with SWIPT, is a likely scheme for 5G and B5G networks because of their high reliability, low latency, and ultra-responsive properties. In [12], the authors proposed the resource allocation algorithm for the simultaneous wireless information and power transfer (SWIPT) multiple carrier NOMA network, considering the pattern division multiple access (PDMA) technique. To keep the quality of service (QoS) at a satisfactory level, the authors have minimized the transmitted power considering the EH scheme. With the ability to link to hundreds or thousands of UEs, new applications and use cases for smart cities, corporate homes, smart farms, smart schools, and families will emerge. DL approaches are an excellent way to address the issues. In [13], the authors provide a full review of how deep neural networks (DNNs) are being employed to address different 5G NOMA receiver issues. To begin, the DNNs used in NOMA are enumerated and described. Following that, their roles are carefully examined to improve NOMA performance. When the SIC is optimal, the bit error rate (BER) performance of NOMA outperforms that of a traditional OFDMA system. A perfect channel state information (CSI) is necessary to complete SIC in the receiver. It is impossible to devise an effective power distribution plan without knowing the precise CSI at the transmitter. It is tough to deal with a perfect or almost perfect CSI. Fortunately, DL techniques have previously been proven to be a feasible answer to this problem. It may be used in NOMA to identify a channel condition that is entirely unknown and time-varying. The decoding of data in a conventional SIC-based NOMA detector is not perfect in the case of a real-time propagation scenario [14], [15]. The DL-based multiple-input multiple-output (MIMO)-NOMA network was examined by the authors in [16]. The authors developed a DL-based SIC detector and precoders for joint optimization using the superposition coding approach in this technique. Because of the receiver's complexity and erroneous transmission of user data, the performance of a traditional SIC is impaired [17], [18]. Because it mitigates frequency selective fading, orthogonal frequency division multiplexing (OFDM) is a vital technology and one of the most well-known modulation methods utilised in the NOMA system [17]. In [19], a DL-based NOMA detector is proposed, based on DNN. The proposed DL NOMA detector perfectly decodes and estimates the originally transmitted user data. The proposed technique improves the BER performance and decreases the overhead of the reference signal to increase the downlink (D/L) NOMA system's data rate and end-to-end reliability. One of the advantages of the proposed technique is that it can process the conventional NOMA data directly instead of designing the SIC-based detector. The advantage of the DNN-based detector is that it can handle large data applications. Furthermore, the NOMA detector is characterized by DNN, which jointly does the signal detection and channel estimation.

In this study, the LSTM algorithm is applied to increase the performance of NOMA systems. The OFDM transmitter and receiver block diagram are shown first, followed by the LSTM algorithm. Then, using the NOMA approach, we examine the DL integration. Finally, we provide a summary of the challenges found while using DL techniques in NOMA. The effect of clipping distortion and nonlinear noise is explained through simulations.

2. SYSTEM MODEL

A. DL basics

Artificial neural networks (ANNs) are motivated by human brain function or, in a larger idea, 5G and B5G information processing applications. ANNs, on the other hand, do not have the same structure as the human brain. Human brains are very complex, dynamic, living creatures that are always changing. ANNs are static and symbolic, unlike the human brain, and making them dynamic is a difficult task. DNNs have several layers, which are referred to as "deep." Data-driven 5G signal processing techniques for difficult communication engineering problems have been demonstrated to be a useful scheme for developing data-driven 5G signal processing techniques. Many assembled algorithms can be overcome by DL algorithms because they recognize the important properties and qualities of the input signals rather than requiring an individual to identify and represent them. DNN [Figure 1] can learn complicated aspects of human-created material such as photographs and audio/video recordings and use them for categorization and decision-making. However, with 5G networks, people provide the information data, the propagation fading channel links are very simple to predict, and we know how to operate near theoretical channel capacity. Is this to say that DL has no place in future communication systems development? Although the answer to the preceding question is "no," we must be cautious not to recreate the wheel for the reasons stated above. We must first identify the issues that DL can solve and then go from there rather than start from scratch. Many complex signal processing problems at the physical layer of 5G wireless networks can be solved optimally by utilizing well-known estimation, detection, and convex optimization (CO) schemes, for example. DL has

been a crucial enabler in 5G, including deep supervised learning (DSL), deep unsupervised learning (DUL), and DRL. Without access to mathematical formulations, DL techniques can solve a broad range of difficulties in 5G networks, such as decision-making, optimization, and prediction, efficiently and effectively, which helps accelerate the design and deployment of wireless communications functionality, especially in situations where mathematical models fail to properly formulate the considered concerns [20], [21], [22]. The application of DL to the 5G network is still in its early stages, and its potential and advantages over well-established mathematical models have yet to be thoroughly investigated and proven. Furthermore, the use of DL schemes in 5G networks raises a slew of issues, including data communication, model design, model training, model deployment, and security protection, all of which must be handled properly [23], [24], [25]. In addition, new challenges for recent 5G scenarios such as radio access networks (RAN), three dimensional (3D) networks, optical wireless communications (OWC), unmanned aerial vehicles (UAVs), and wireless power transfer (WPT) will include 5G wireless network functional modules and high-performance requirements. The development of DL-based solutions to meet traditional 5G network requirements has recently been shown to have a lot of potential for breaking the bottleneck in traditional 5G networks. In the paper [22], [26], [27], we investigate the use of DL in 5G NOMA, including physical layer processing and resource allocation. In a typical 5G network, DL can improve the BER performance of each (traditional) block or optimize the entire transmitter or receiver at the same time. Therefore, we can distinguish between DL applications that employ block processing structures and those that do not in 5G and B5G physical layer communications. For signal detection in DL-based 5G and B5G networks with block topologies, we deliver integrated CSI and signal identification based on a fully linked DNN, model-driven DL [28], [29], [30], [22]. We present our latest efforts in constructing end-to-end learning communication systems using DRL and generative adversarial networks (GANs) for those without block structures. 5G and B5G communication networks may be made more efficient through judicious resource (spectrum, power, etc.) allocation. Conventional insight is that optimal power allocation (OPA) should be formulated as a CO problem, with mathematical programming used to solve it to a specific level optimally [31], [32], [33], [34], [35]. Because of its exceptional ability to harness data for problem-solving, DL is a viable option. It can assist in solving resource allocation optimization concerns or be used directly for resource allocation. In work [36], the authors show how to utilize DL to simplify MINLP. The authors will next go into how to use DRL directly for wireless resource allocation in V2V networks by employing applications. In 5G NOMA networks, selective fading of the recurrent neural network (RNN) and nonlinear LSTM were investigated for nonlinear time prediction and modeling. The authors in [37] studied current LSTM cell derivatives and network designs for time series prediction. RNN and LSTM techniques are used in sectors like as computer vision, blockchain technology, Covid-2019 prediction and analysis, VR, AR, and Natural Language Processing, with outcomes that are comparable to, if not better than, classical algorithms. Its popularity stems from the fact that it is simple to use and outperforms other popular activation functions such as Sigmoid and Tanh. Gradient disappearance is less likely to interfere with DL fading channel model training, but other problems such as saturated and "dead" units can occur.The following is the formula for calculating the Sigmoid activation function: $1/(1+\exp(-x)).1/(1+\exp(-x))$. Where e is a well-defined constant value that serves as the foundation for the natural logarithm. Tanh is the abbreviation for the hyperbolic tangent activation function. The S-shape of the sigmoid activation function is quite like that of the sigmoid activation function. Any real value can be used as an input, and the function returns a value between -1 and 1. The input is closer to 1.0, the output is closer to -1.0, and the input is smaller than -1.0. The following formula may be used to determine the Tanh activation function: $(e(x)-e(-x))/(e(x)+e(-x))$. The base of the natural logarithm is e, which is a mathematical constant. Work [17] provides a comprehensive examination of DL. The DNN [17] is depicted in Figure 2 as a Gray box.

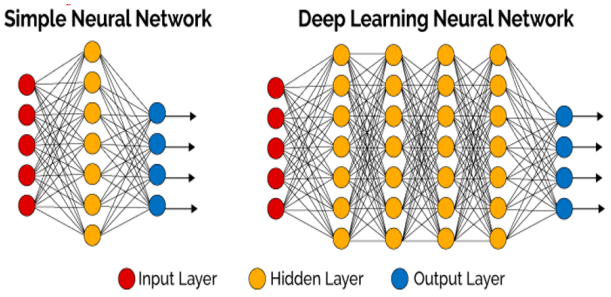

Figure 1. Schematic representation of the DNN [17].

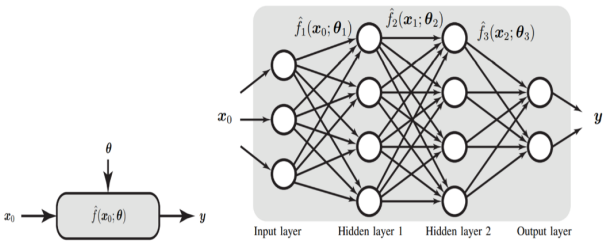

(a) (b)

Figure 2. (a) Gray box model representation with output y and input x_0. (b) The Gray-box input-output model is defined by $\hat{f}$ and a parameter vector θ. (i) It $\hat{f}$ is referred to as an ANN (ii) when it has a complicated shape, such as the one shown in it [17].

B. *OFDM system arichtecture*

Figure 3 depicts the OFDM transmitter and receiver in block diagram form. The quadrature phase-shift keying (QPSK) modulation algorithm is used to create the digitally modulated symbols. First, utilizing serial to parallel (SP)

transmission process, the data symbols are transformed to a parallel data stream. The data symbols are in the frequency domain (FD), and the inverse FT method is used to transfer them to the time domain (TD). The CP length is greater than

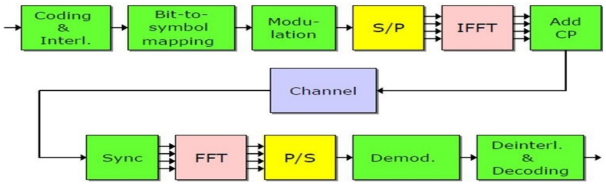

Figure 3. Block diagram representation of the OFDM transmitter and receiver [20].

the maximum value of the delay spread, which is used to reduce fading and eliminate frequency selective fading (also known as inter-symbol interference (ISI)). Let us consider $\left\{\sum_{t=0}^{L-1} b(t)\right\}$ represents the multi-tap channel. The received signal $r(t)$ is represented as [38], [39], [40],

$$r(k) = g(k) \otimes b(k) + \mathrm{z}(k), \tag{1}$$

$\otimes$ stands for circular convolution, whereas $g(k)$ and $\mathrm{z}(t)$ stand for transmitted signal and AWGN noise, respectively. The resultant signal is expressed in (8) after the CP has been removed from the receiver side and the discrete FT has been performed on the expression given in (7) [38], [39], [41], [40], [42],

$$R(J) = G(J)N(J) + Z(J), \tag{2}$$

The discrete Fourier transform (DFT) of $r(k), g(k), b(k)$, and $\mathrm{z}(k)$, are $R(J), G(J), N(J)$, and $Z(J)$, respectively. In this paper, we look at a two-user NOMA-OFDM system, where both users are expected to send data at the same time since they share the same frequency resources. A two-user NOMA system is depicted schematically in Figure 4 [41], [40], [42]. Both user signals are superimposed at the base station (BS) in the uplink (U/L) NOMA system, yielding the expression [38], [39], [41], [40], [43], [44], [45].

$$R(J) = \sum_{n=1}^{M} \sqrt{P_n(J)} G_n(J) N_n(J) + Z(J), \tag{3}$$

where $Z(J), G_n(J)$, and $R(J)$ denote AWGN channel noise, transmitted OFDM symbol, and FD received signal, respectively. On the J^{th} subcarrier, the n^{th} user's power is represented as $P_n(J)$. For M number of subcarriers, the total transmitted power is denoted by P. The power is distributed based on the value of the power allocation factors, which are denoted by the letters

$$\beta_n(J) = \frac{P_n(J)}{P},$$

for the n^{th} user. The entire quantity of accessible power is limited, and this limitation is symbolized by the letter $\sum_{n=1}^{M} \beta_n(J) = 1$. Because of multipath propagation, the channel is multitap, and the channel impulse response is $b_n(q) = \sum_{l=1}^{L} \kappa_{n,l} \varsigma(q - \omega_{n,l})$ with complex channel gain $\kappa_{n,l}$ and time delay of the l^{th} multi-path for the i^{th} user $\omega_{n,l}$. $b(q)'s$ DFT is $N_n(J)$. There are 20 total determined pathways, and fading linkages are Rayleigh distributed [41], [40].

3. DL-BASED NOMA RECEIVER

A. LSTM Network

The RNN approach is a subset of the LSTM algorithm [Figure 5], which has five layers. The input layer is the initial layer, followed by the LSTM layer, the SoftMax layer, and finally the classification layer. Because it can use data time-dependence, the LSTM NOMA layer, a kind of RNN, is a core component of the DNN and is often employed for the classification of sequence and time-series data. The data is held by the LSTM algorithm, which learns it in a series of stages. OFDM subcarriers are shown as time steps using NOMA DL detectors that employ the LSTM algorithm. The DNN network is trained to realize the multi-user IDs of a particular subcarrier by focussing on the single time step module provided by the LSTM layer.

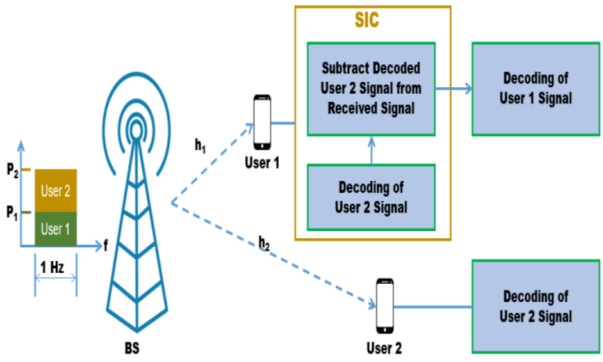

Figure 4. Two-user NOMA system

B. NOMA-OFDM DL Model Training

Consider a 72-subcarrier OFDM system with packetized data. For the purpose of simplicity, a packet is made up of three OFDM signals. Two pilot sequences are provided for each user, each filling the first two OFDM symbols and the 3rd OFDM symbol containing the data stream. It contains the first two OFDM symbols and the 3rd OFDM symbol contains individual data sequences. QPSK uses the digital modulation technique to create OFDM data symbols, each with a two-bit/subcarrier QPSK symbol. The OFDM data packet is made up of three QPSK data symbols that are generated at random with a fixed pilot symbol [41], [40].The FD OFDM symbol is transformed into the TD OFDM symbol by inserting CP as a guarding time gap between two OFDM signals. An OFDM packet is made up of three QPSK data symbols and one fixed pilot symbol, with the QPSK symbols generated at random. For converting FD OFDM symbols to TD OFDM symbols, the CP between two OFDM signals serves as the guard time

interval. CP helps to attenuate the ISI impact by decreasing the effects of the fading channel [29-30]. To avoid the ISI effect, the channel impulse response needs to be shorter than the CP length. The dimension of the feature vector is equal to 72×3×2= 432 if there are 72 sub-carriers and 3 symbols. The DNN will be trained to find the data symbols for the k-th subcarrier if the matching label $Xi(k)$ is assigned during training. A label is a number that simultaneously reflects both users' equipment's sent data symbols. Because every user device sends QPSK data symbols, there will be 16 combinations/labels, i.e., [41], [40]. The length of the real-valued vector, which is 432, determines the input vector's dimension. QPSK data is sent by all user equipment. There are a lot of hidden layers, a total of 128, because we're using DNN, and the fully connected layer with an output size of 16 comes after them. The projected $Xi(k)$ mark will be created by the classification layer, and the SoftMax layer will add a SoftMax function to its input to map all data symbols given by user equipment all at once by the SoftMax layer.

4. SIMULATION RESULTS

This section uses simulations to show how the DL approaches for symbol identification and channel estimation in the NOMA OFDM system function from start to finish. The simulation data will be utilized to train the NOMA OFDM DL detector, and the NOMA OFDM DL detector's performance in terms of BER will be compared to that of traditional NOMA receivers over a range of SNR regimes. In simulations, the DL-based solution outperforms the LSE and MMSE methods. The CP is eliminated, or nonlinear clipping noise occurs when fewer training pilots are used. The number of subcarriers and the length of CP in our simulation are 72 and 16, respectively. The carrier frequency is 2.6 GHz, and there are 24 different routes to choose from. The urban channel is used, with a maximum delay spread of 16 and QPSK complex modulating symbols.

A. Calculation of the effect of the number of Pilot Numbers on the BER Performance

The standard SIC-based receivers, such as LSE and MMSE, were compared to the DL-based NOMA receiver in terms of BER performance. Because the fading channel's 2nd order data statistics are expected to be known and may be utilized to detect OFDM data symbols, the LSE receiver performs the worst, while the MMSE performs substantially better. The DL-based NOMA channel estimator and detector outperform the LSE approach and are comparable to the MMSE methodology in terms of outage and BER. In simulations, 16 sample periods have been considered, with a lesser number of pilot symbols are used for improving the SE. When just 12 pilot symbols are included, the BER performance is worse than when 72 pilot symbols are considered. The DNN's input and output will be the same for both 72 and 12 pilot symbols [41]. When the SNR is almost equal to 9 dB, the BER SIC-based LSE and MMSE methods are shown to be consistent. Furthermore, the simulation curves demonstrate that when the value of SNR increases, the BER of the DL scheme reduces dramatically, implying that the DL NOMA detector is robust and independent of the number of pilot symbols employed for OFDM signal detection [19], [41], [40]. The superior performance of the DL-based NOMA channel estimator and detector may be described by investigating the fading channel coefficients based on the training data symbols provided by the DL NOMA model [4], [5], [41], [40].

B. The Impact of the CP on end-to-end BER performance

CP is utilised to reduce ISI and adjacent channel interference (ACI), as well as to help with the conversion of linear to circular convolution and offer OFDM signal resiliency. The BER performance comparison with and without CP is shown in Figure 7.

Neither MMSE nor LSE can offer correct fading channel

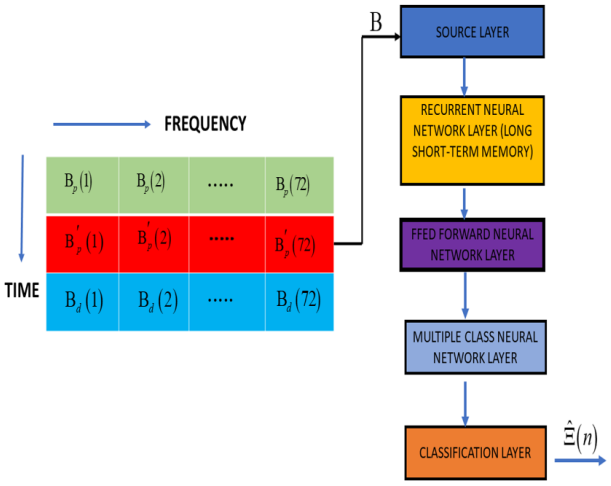

Figure 5. Schematic representation of the LSTM-based DL model [4], [5], [41], [40].

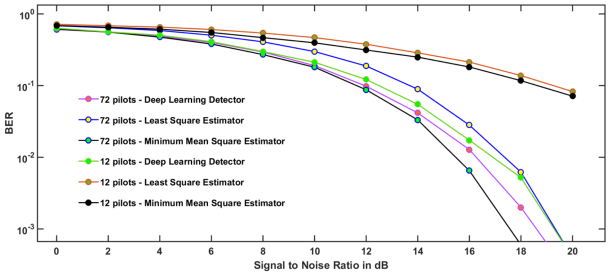

Figure 6. BER vs SNR charts of the DL NOMA detector for 72 and 12 pilot symbols, respectively.

coefficient information. Precision tends to be saturated at SNR levels above 15 dB. On the other hand, DL approaches remain effective in channel estimation and detection. This finding demonstrates that the wireless fading channel's potential has been revealed and that DNNs in the training stage is capable of mastering it. Impact of BER performance due to clipping distortion OFDM's main drawbacks are its

high PAPR and sensitivity to frequency offset and phase noise. Clipping is one of the methods for dealing with the PAPR problem. We experience non-linear noise after the clipping procedure is completed, which lowers system performance.

$$\hat{\Psi}(k) = \begin{cases} \Psi(k), & if\ |\Psi(k)| \le \Theta \\ \Theta \exp(-j\varphi(k)), & otherwise \end{cases} \quad (4)$$

$\varphi(k)$ and Θ represent the phase shift and threshold, respectively. When the DL NOMA network is exposed to nonlinear noise, Figure 8 shows the BER and outage probability performance of standard SIC-based detectors (MMSE and LSE). The graphs show that for clipping ratio 1, the DL-NOMA channel estimator and detector outperform the SIC detectors for SNR ¿ 15dB, assuming that the DL scheme is more robust to PAPR problems caused by clipping. Figure 9 shows a comparison of the SIC and DL channel estimators and detectors for all practical fading channel conditions, except for CP and clipping distortion. Even though the NOMA detector based on DL is more efficient than ordinary detectors, there is a difference in detection performance under ideal conditions, as we showed before.

C. Robustness Analysis

The channel coefficients are calculated online with data sets that are like those used in offline training. In real-time propagation circumstances, however, there is a latency between offline and online deployment. It is also important that these mismatches stay consistent long enough for the trained models to work. Figure 10 depicts the impact of frequency selective fading on the fading relationship statistics utilized in the training and testing stages. The maximum delay spread and the number of multipath in the testing stage are shown to be different from those in the training stage. The efficacy of data symbol identification is unaffected by changes in fading connections data statistics in Figure 10.

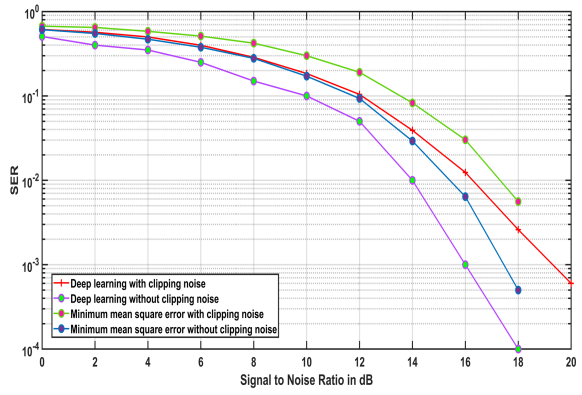

Figure 7. BER vs SNR charts of the DL NOMA detector [CN-Clipping Noise] with and without clipping noise.

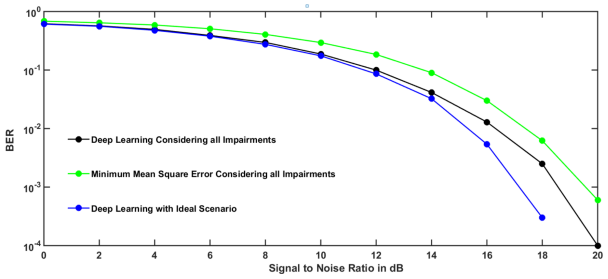

Figure 8. BER plots considering all feasible scenarios.

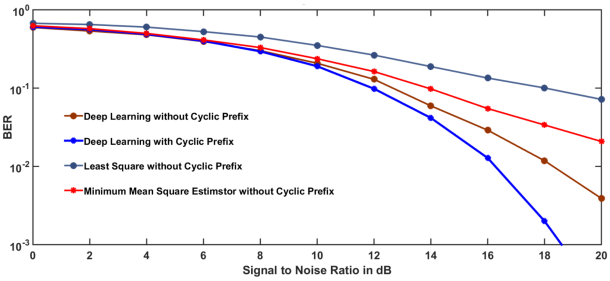

Figure 9. Plots of BER against SNR for the DL NOMA detector with and without the CP, $CP = 16$.

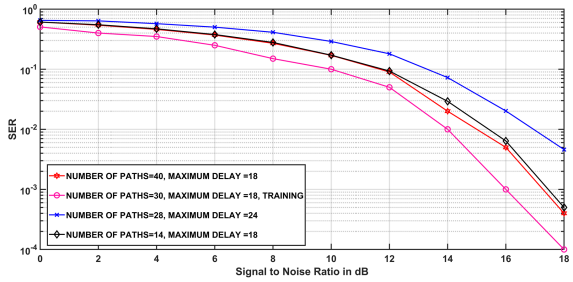

Figure 10. BER charts that account for the time lag between deployment and training processes.

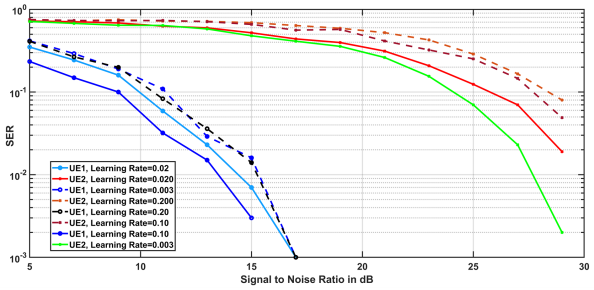

Figure 11. BER graphs of the DL NOMA detector for various learning rate values.

D. Impact of learning rate

In Figure 11, the BER versus SNR in dB is plotted for both users, the BER vs SNR in dB is presented in Figure 11 for various learning rates. Simulated results show that lower learning rates improve BER performance substantially, but a high learning rate causes fast weight

TABLE I. Simulation Parameters

Number of Subcarriers	72	Number of training data	500000
Number of pilot subcarriers	72 and 12	Number of DNN layers	5
Channel length	20	Number of Epochs	150
Cyclic prefix length	20	Learning Rate	0.02
Total number of NOMA users	02	Batch Size	25000

TABLE II. System Parameters ReLU

Parameter Value	Value
OS	Windows 10
Framework	TensorFlow
Coding	Python 3.5 and MATLAB
Fading links	MIMO channel and AWGN fading channel
Channel fading	Rayleigh Distribution
Number of user devices per cluster	2
Number of antennas equipped at the transmitter	4
Number of antennas equipped at the receiver	4
Modulation symbols	QPSK
Number of training samples	409,600
Total transmitted power per antenna	2W
Power allocation factor	0.80
Hidden layer	ReLU

changes in the DL NOMA detector, resulting in a very high validation error value. It is possible that a slower learning rate will result in extraordinarily high accuracy. However, the enormous number of iterations is necessary due to the sluggish convergence rate. While a lower learning rate, such as 0.003, improves accuracy, it slows convergence since it necessitates more adjustments. The learning threshold for all other simulation instances has been adjusted at 0.02 as a trade-off between testing accuracy and training time.

5. CONCLUSION

In this article, traditional SIC NOMA approaches are compared to the performance of a DL-based NOMA-OFDM system. Neither the MMSE nor the LSE can offer exact information on fading channel coefficients. Standard SIC-based receivers, such as LSE and MMSE, are compared with NOMA DL-based receivers in terms of BER performance. Since the quadratic data statistics of the fading channel are assumed to be known and can be used to detect OFDM data symbols, the LSE receiver performs worse, while the MMSE performs significantly better. The DL-based NOMA channel detector and estimator perform better than the LSE approach and are comparable to the MMSE scheme in terms of error and BER. Low learning rates increase system performance. However, high learning rates cause rapid changes in the DL NOMA detector's weights, resulting in a very high validation error value. For all other simulation scenarios, the learning level has been set at 0.02 to balance the trade-off between testing precision and training time.

REFERENCES

[1] S. Pandya, M. A. Wakchaure, R. Shankar, and J. R. Annam, "Analysis of noma-ofdm 5g wireless system using deep neural network," *The Journal of Defense Modeling and Simulation*, March 2021. [Online]. Available: https://doi.org/10.1177/1548512921999108

[2] L. Bhardwaj, R. K. Mishra, and R. Shankar, "Sum rate capacity of non-orthogonal multiple access schemes with optimal power allocation," *The Journal of Defense Modeling and Simulation*, Jan. 2021.

[3] B. P. Chaudhary, R. Shankar, and R. K. Mishra, "A tutorial on cooperative non-orthogonal multiple access networks," *The Journal of Defense Modeling and Simulation*, Feb. 2021.

[4] R. Shankar and R. K. Mishra, "An investigation of s-df cooperative communication protocol over keyhole fading channel," *Physical Communication, Elsevier*, vol. 29, pp. 120–140, 2018.

[5] R. Shankar, "Examination of a non-orthogonal multiple access scheme for next-generation wireless networks," *The Journal of Defense Modeling and Simulation*, sep 2020.

[6] B. Lokesh, R. K. Mishra, and R. Shankar, "Examination of outage probability for next-generation nonorthogonal multiple access scheme in uplink and downlink scenario," *In 2019 IEEE International Symposium on Signal Processing and Information Technology (ISSPIT)*, pp. 1–5, 2019.

[7] R. Shankar and R. K. Mishra, "S-df cooperative communication system over time selective fading channels," *Journal of Information Science Engineering*, vol. 35, no. 6, 2019.

[8] A. Yarali, "Ai, 5g, and iot," *Intelligent Connectivity: AI, IoT, and 5G , IEEE*, pp. 117–131, 2022.

[9] E. hajj M., F. A., C. M., and Serhrouchni, "A survey of internet of things (iot) authentication schemes," *Sensors*, vol. 19, p. 1141, 2019.

[10] Peiro, Paloma, C. Q. G. Muñoz, and F. P. GarcíaMárquez, "Use of uavs, computer vision, and iot for traffic analysis," *Internet of Things*, pp. 275–296, 2021.

[11] J. Gozalvez, "Samsung electronics sets 5g speed record at 7.5 gbs [mobile radio," *IEEE Vehicular Technology Magazine*, vol. 10, no. 1, pp. 12–16, 2015.

[12] B. M. Kumar, R. Shankar, and S. S. Singh, "Analysis of the energy harvesting non-orthogonal multiple access technique for defense applications over rayleigh fading channel conditions," *Journal of Defense Modeling and Simulation*, july 2021.

[13] M. K. Hasan, M. Shahjalal, M. M. Islam, M. M. Alam, M. F. Ahmed, and Y. M. Jang, "The role of deep learning in noma for 5g and beyond communications," *2020 International Conference on Artificial Intelligence in Information and Communication (ICAIIC)*, pp. 303–307, 2020.

[14] M. R. Usman, A. Khan, M. A. Usman, Y. S. Jang, and S. Y. Shin, "On the performance of perfect and imperfect sic in downlink nonorthogonal multiple access (noma)," *2016 International Conference on Smart Green Technology in Electrical and Information Systems (ICSGTEIS)*, pp. 102–106, 2016.

[15] M. R. Usman and S. Y. Shin, "Channel allocation schemes for permanent user channel assignment in wireless cellular networks," *IETE Journal of Research*, vol. 62, no. 2, pp. 189–197, 2016.

[16] C. Lin, Q. Chang, and X. Li, "A deep learning approach for mimo-noma downlink signal detection," *Sensors*, vol. 19, no. 11, p. 2526, 2019.

[17] S. Ravi, S. BK, M. H, K. AS, N. R, and S. B. A., "Impact of the learning rate and batch size on noma system using lstm-based deep neural network," *The Journal of Defense Modeling and Simulation*, oct 2021.

[18] A.-B. Joel, R. Shankar, P. Krishna, and S. K. S., "Investigation of bi-directional lstm deep learning-based ubiquitous mimo uplink noma detection for military application considering robust channel conditions," *The Journal of Defense Modeling and Simulation*, oct 2021.

[19] R. Shankar, T. V. Ramana, P. Singh, S. Gupta, and H. Mehraj, "Examination of the non-orthogonal multiple access system using long short memory based deep neural network," *Journal of Mobile Multimedia*, pp. 451–474, 2021.

[20] H. Hewamalage, C. Bergmeir, and K. Bandara, "Recurrent neural networks for time series forecasting: Current status and future directions," *International Journal of Forecasting*, vol. 37, pp. 388–427, 2021,https://doi.org/10.1016/j.ijforecast.2020.06.008.

[21] Dey, Prasanjit, C. Kumar, M. Mitra, R. Mishra, S. K. Chaulya, G. M. Prasad, S. K. Mandal, and G. Banerjee, "Deep convolutional neural network based secure wireless voice communication for underground mines," *Journal of Ambient Intelligence and Humanized Computing*, pp. 1–20, 2021.

[22] E. Björnson and P. Giselsson, "Two applications of deep learning in the physical layer of communication systems." *arXiv preprint arXiv:2001.03350*, 2020.

[23] M. Elwekeil, S. Jiang, T. Wang, and S. Zhang, "Deep convolutional neural networks for link adaptations in mimo-ofdm wireless systems," *IEEE Wireless Communications Letters*, vol. 8, no. 3, pp. 665–668, june 2019.

[24] Islam, S. Riazul, M. Zeng, O. A. Dobre, and K. Kwak, "Nonorthogonal multiple access (noma): How it meets 5g and beyond," *Wiley 5G Ref: The Essential 5G Reference Online*, pp. 1–28, 2019.

[25] S. Wang, R. Yao, T. A. Tsiftsis, N. I. Miridakis, and N. Qi, "Signal detection in uplink time-varying ofdm systems using rnn with bidirectional lstm," *IEEE Wireless Communications Letters*, vol. 9, no. 11, pp. 1947–1951, nov 2020.

[26] S. Kojima, K. Maruta, and C. Ahn, "Adaptive modulation and coding using neural network based snr estimation," *IEEE Access*, vol. 7, pp. 183 545–183 553, 2019.

[27] C. HB, A. Almadhor, and K. W., "Machine learning for 5g mimo modulation detection," *Sensors*, vol. 21, no. 5, p. 1556, feb 24 2021.

[28] S.-C.-K. Kalla, C. Gagné, M. Zeng, and L. A. Rusch, "Recurrent neural networks achieving mlse performance for optical channel equalization," *Opt. Express*, vol. 29, pp. 13 033–13 047, 2021.

[29] X. Zhu, Z. Sheng, and Y. Fang, "A deep learning-aided temporal spectral channelnet for ieee 802.11p-based channel estimation in vehicular communications," *J Wireless Com Network*, vol. 94, 2020.

[30] Ashish, I. Kumar, and R. K. Mishra, "Performance analysis for wireless non-orthogonal multiple access downlink systems," *2020 International Conference on Emerging Frontiers in Electrical and Electronic Technologies (ICEFEET)*, pp. 1–6, 2020.

[31] S. Singh, D. Mitra, and R. K. Baghel, "Analysis of noma for future cellular communication," *2019 3rd International Conference on Trends in Electronics and Informatics (ICOEI)*, pp. 389–395, 2019.

[32] Erpek, Tugba, T. J. O'Shea, Y. E. Sagduyu, Y. Shi, and T. C. Clancy, "Deep learning for wireless communications," *Development and Analysis of Deep Learning Architectures, Springer*, pp. 223–266, 2020.

[33] Shoeibi and A. et al., "Epileptic seizures detection using deep learning techniques: A review," *International journal of environmental research and public health*, vol. 18, no. 11, p. 5780, 2021.

[34] A. Zappone, M. D. Renzo, and M. Debbah, "Wireless networks design in the era of deep learning: Model-based, ai-based, or both?" *IEEE Transactions on Communications*, vol. 67, no. 10, pp. 7331–7376, oct 2019.

[35] S. Thota, Y. Kamatham, and C. S. Paidimarry, "Analysis of hybrid papr reduction methods of ofdm signal for hpa models in wireless communications," *IEEE Access*, vol. 8, no. 10, pp. 22 780–22 791, 2020.

[36] Z. Mlika and S. Cherkaoui, "Network slicing for vehicular communications: a multi-agent deep reinforcement learning approach," *Ann. Telecommun*, vol. 76, pp. 665–683, 2021.

[37] S. Dargan, M. Kumar, Ayyagari, and M. et al, "A survey of deep learning and its applications: A new paradigm to machine learning," *Arch Computat Methods Eng*, vol. 27, p. 1071–1092, 2020.

[38] A. A. Khansa, Y. Yin, G. Gui, and H. Sari, "Power-domain noma

or noma-2000?" *25th Asia-Pacific Conference on Communications*, pp. 336–341, 2019.

[39] M. K. Simon and M. Alouini, "Digital communications over fading channels (m.k. simon and m.s. alouini; 2005) [book review]," *IEEE Transactions on Information Theory*, vol. 54, no. 7, pp. 3369–3370, july 2008.

[40] Narengerile, "Deep learning for signal detection in noma systems (https://www.mathworks.com/matlabcentral/fileexchange/75478-deep-learning-for-signal-detection-in-noma-systems," *MATLAB Central File Exchange*, july 19 2021.

[41] Narengerile and J. Thompson, "Deep learning for signal detection in non-orthogonal multiple access wireless systems," *2019 UK/ China Emerging Technologies (UCET)*, pp. 1–4, july 2019.

[42] R. Tiwari and S. Deshmukh, "Prior information-based bayesian mmse estimation of velocity in hetnets," *IEEE Wireless Communications Letters*, vol. 8, no. 1, pp. 81–84, feb 2019.

[43] S. Shrivastava, R. Tiwari, and S. Das, "Comparative performance evaluation of a new dynamic-double-threshold energy detection scheme with basic spectrum sensing techniques," *2014 International Conference on Green Computing Communication and Electrical Engineering (ICGCCEE)*, pp. 1–6, 2014.

[44] R. Tiwari, S. Shrivastava, and S. Das, "Performance analysis of patient monitoring system under different routing algorithm," *International Conference for Convergence for Technology-2014*, pp. 1–6, 2014.

[45] R. Tiwari and S. Deshmukh, "Mvu estimate of user velocity via gamma distributed handover count in hetnets," *IEEE Communications Letters*, vol. 23, no. 3, pp. 482–485, march 2019.

Dr. Abhishek Bhatt is an associate professor in the Department of Electronics and Telecommunication Engineering at the College of Engineering Pune (COEP). He received his B.Tech in Electronics and Communication and M.Tech in Digital Communication during 2003 and 2008, respectively, and his Ph.D. degree in Image Processing and remote sensing from the Indian Institute of Technology Roorkee in 2016. He is the author of more than 50 journal/Conference papers and has written one book in signal processing using MATLAB. His current research interests include Image/Signal Processing, Computer Vision, Antenna wave propagation and Electromagnetic Field Theory.

Ravi Shankar received his BE degree in Electronics and Communication Engineering from Jiwaji University, Gwalior, India, in 2006. He received his MTech degree in Electronics and Communication Engineering from GGSIPU, New Delhi, India, in 2012. He received a PhD in Wireless Communication from the National Institute of Technology Patna, Patna, India, in 2019. He was an assistant professor at MRCE Faridabad, from 2013 to 2014, where he was engaged in researching wireless communication networks. His current research interests cover cooperative communication, D2D communication, IoT/M2M networks and networks protocols. He is a student member of IEEE.

Gniewko Niedbała is scientific researcher in academic level and associate professor in agriculture, applied informatics and machine learning. Professional activity: 2012-2016 Member of the Board of the National Centre for Research and Development, Poland. Research activity started in 2006 resulted in the publication of specialized books as author and / or co-author (published abroad), over 100 scientific articles (of which 40 in foreign journals / conferences). Associate member of networks, research institutions and scientific journals.

Ajay Rupani received his B. Tech. degree in Electronics and Communication Engineering from Jodhpur Institute of Engineering Technology, Jodhpur, India in 2012. He received his M. Tech. degree in VLSI Design from Rajasthan Institute of Engineering Technology, Jaipur, India in 2017. He has seven years of teaching experience. At present, He is pursuing PhD in Electronics and Communication Engineering from Manipal University, Jaipur. His current research interests are VLSI Design, Machine Learning and Wireless Communication for the networks. He is a professional member of the IEEE.